# The EGFRvIII transcriptome in glioblastoma

Hoogstrate, Youri; Ghisai, Santoesha A; de Wit, Maurice; de Heer, Iris; Draaisma, Kaspar; van Riet, Job; van de Werken, Harmen J G; Bours, Vincent; Buter, Jan; Vanden Bempt, Isabelle

*Published in:*
Neuro-Oncology

*DOI:*
10.1093/neuonc/noab231

Neuro-Oncology

24(3), 429–441, 2022 | https://doi.org/10.1093/neuonc/noab231 | Advance Access date 5 October 2021



# The *EGFRvIII* transcriptome in glioblastoma: A meta-omics analysis

**Youri Hoogstrate, Santoesha A. Ghisai, Maurice de Wit, Iris de Heer, Kaspar Draaisma, Job van Riet, Harmen J. G. van de Werken, Vincent Bours, Jan Buter, Isabelle Vanden Bempt, Marica Eoli, Enrico Franceschi, Jean-Sebastien Frenel, Thierry Gorlia, Monique C. Hanse, Ann Hoeben, Melissa Kerkhof, Johan M. Kros, Sieger Leenstra, Giuseppe Lombardi, Slávka Lukacova, Pierre A. Robe, Juan M. Sepulveda, Walter Taal, Martin Taphoorn, René M. Vernhout, Annemiek M. E. Walenkamp, Colin Watts, Michael Weller, Filip Y. F. de Vos, Guido W. Jenster, Martin van den Bent, and Pim J. French**

*Department of Neurology, Erasmus MC, Rotterdam, The Netherlands (Y.H., S.A.G, M.d.W, I.d.H., M.v.d.B., W.T., P.J.F); Cancer Computational Biology Center, Erasmus MC, Rotterdam, The Netherlands (Y.H., J.v.R., H.J.G.v.d.W.); Department of Urology, Erasmus MC, Rotterdam, The Netherlands (Y.H., H.J.G.v.d.W., G.W.J.); Department of Neurosurgery, UMC Utrecht, Utrecht, The Netherlands (K.D., P.A.R.); Department of Medical Oncology, Erasmus MC, Rotterdam, The Netherlands (J.v.R.); Department of Pathology, Erasmus MC, Rotterdam, The Netherlands (J.M.K., M.E.v.R.); Department of Immunology, Erasmus MC, Rotterdam, The Netherlands (H.J.G.v.d.W.); Department of Human Genetics, Université de Liège, Liège, Belgium (V.B.); Department of Oncology, VU University Medical Center, Amsterdam, The Netherlands (J.B.); Department of Human Genetics, University Hospitals Leuven, Leuven, Belgium (I.V.B.); Unit of Molecular Neuro-Oncology, Besta-IRCCS, Milan, Italy (M.E.); IRCCS Istituto Scienze Neurologiche di Bologna, Nervous System Medical Oncology Department, Bologna, Italy (E.F.); Institut de Cancérologie de l'Ouest, Nantes, France (J-S.S.F); EORTC Headquarters, Brussels, Belgium (T.G.); Department of Neurology, Catharina Hospital, Eindhoven, The Netherlands (M.C.H.); Department of Medical Oncology, Maastricht UMC+, Maastricht, The Netherlands (A.H.); Department of Neurology, Haaglanden Medical Center, The Hague, The Netherlands (M.K., M.T.); Department of Neurosurgery, Erasmus MC, Rotterdam, The Netherlands (S.L.); Veneto Institute of Oncology IOV-IRCCS, Padua, Italy (G.L.); Department of Oncology, Aarhus University Hospital, Aarhus, Denmark (S.L.); Hospital Universitario 12 de Octubre, Madrid, Spain (J.M.S.); Department of Radiotherapy, Erasmus MC, Rotterdam, The Netherlands (R.M.V.); Department of Medical Oncology, UMC Groningen, Groningen, The Netherlands (A.M.E.W.); Institute of Cancer and Genomic Sciences, University of Birmingham, Birmingham, United Kingdom (C.W.); Department of Neurology, University Hospital Zurich, Zurich, Switzerland (M.W.); Department of Medical Oncology, UMC Utrecht, Utrecht, The Netherlands (F.Y.F.d.V.)*

**Corresponding Author:** Youri Hoogstrate, PhD, Department of Neurology, Erasmus MC, PO Box 2040, 3000CA Rotterdam, the Netherlands (y.hoogstrate@erasmusmc.nl).

**Abstract**

**Background.** *EGFR* is among the genes most frequently altered in glioblastoma, with exons 2-7 deletions (*EGFRvIII*) being among its most common genomic mutations. There are conflicting reports about its prognostic role and it remains unclear whether and how it differs in signaling compared with wildtype *EGFR*.

**Methods.** To better understand the oncogenic role of *EGFRvIII*, we leveraged 4 large datasets into 1 large glioblastoma transcriptome dataset (n = 741) alongside 81 whole-genome samples from 2 datasets.

**Results.** The *EGFRvIII/EGFR* expression ratios differ strongly between tumors and range from 1% to 95%. Interestingly, the slope of relative *EGFRvIII* expression is near-linear, which argues against a more positive selection pressure than *EGFR* wildtype. An absence of selection pressure is also suggested by the similar survival between *EGFRvIII*-positive and -negative glioblastoma patients. *EGFRvIII* levels are inversely correlated with pan-*EGFR* (all wildtype and mutant variants) expression, which indicates that *EGFRvIII* has a higher potency in downstream pathway activation. *EGFRvIII*-positive glioblastomas have a lower *CDK4* or *MDM2* amplification incidence than *EGFRvIII*-negative ($P$ = .007), which may point toward crosstalk between these pathways. *EGFRvIII*-expressing tumors have an upregulation of "classical" subtype genes compared to those with *EGFR*-amplification

only ($P = 3.873e^{-6}$). Genomic breakpoints of the *EGFRvIII* deletions have a preference toward the 3′-end of the large intron-1. These preferred breakpoints preserve a cryptic exon resulting in a novel *EGFRvIII* variant and preserve an intronic enhancer.

**Conclusions.** These data provide deeper insights into the complex *EGFRvIII* biology and provide new insights for targeting *EGFRvIII* mutated tumors.

### Key Points

- *CDK4* and *MDM2* amplifications appear less frequently in *EGFRvIII*+ compared with *EGFRvIII*– but *EGFR*-amplified GBM.
- Transcriptomes of *EGFR*-amplified GBM differ marginally between *EGFRvIII*+ and *EGFRvIII*–.
- *EGFRvIII* breakpoints preferentially retain an intronic enhancer.

## Importance of the Study

Glioblastoma is the most prevalent and aggressive form of malignant primary brain tumors, often characterized by EGFR mutations for which no effective treatments is available. We aimed to understand the role of its most common mutation, *EGFRvIII* (in-frame deletion of exons 2-7). By exploiting 6 combined datasets, we show the interplay between pan-*EGFR* and *EGFRvIII* levels, find no positive selection towards *EGFRvIII* expression and demonstrate that *EGFRwt* and *EGFRvIII* largely activate similar pathways. However, significant and unique *EGFRvIII* mutation-specific associations were found with Cell Cycle (eg, *CDK4*) and RTK/RAS/PI3K genes (eg, *MDM2*) which provide new insights for tumor targeting. A preference in breakpoint location in intron-1 not only results in a distinct variant of *EGFRvIII* but also preserves an enhancer region, and so provides new insights into *EGFR(vIII)* gene regulation.

Glioblastoma is the most prevalent and aggressive form of malignant primary brain tumor in adults with a short median survival time of 14.6 months.[1] Extensive research on the genetic makeup of glioblastoma has revealed recurrent genetic changes typically involving the RTK/RAS/PI3K, p53, and RB signaling pathways.[2–4] Although the diverse genetic features of glioblastoma have become increasingly better understood, no effective treatment options are currently available that specifically target the most common mutations. One of the most frequently altered genes in glioblastoma encodes the epidermal growth factor receptor (*EGFR*). *EGFR* is amplified in ~50% of all glioblastomas,[4–7] typically within small circular extrachromosomal DNA (ecDNA) copies.[8] The most common mutation on top of this amplification is an in-frame deletion of exons 2-7 (*EGFRvIII*), found in ~50% of the *EGFR*-amplified glioblastoma patients.[9] EGFRvIII is a constitutively, but low-level, active form of EGFR that is independent of ligand for its activation,[9] likely due to the partially deleted extracellular ligand-binding receptor domain. The *EGFRvIII* variant results from a genomic deletion, not from alternative or aberrant splicing. Unfortunately, treatments aimed at targeting *EGFRvIII* have thus far not provided clinical benefit to patients.[10,11]

It is assumed that *EGFRvIII* typically is a late event that arises after chromosome 7 amplification and after *EGFR* high-copy amplifications and is therefore considered subclonal.[12] However, even as subclonal mutation, it is highly prevalent in glioblastoma and contributes to and alters the biology of the tumor. *EGFRvIII* has been shown to reduce apoptosis and increase proliferation and invasiveness,[9] key features of tumor progression. Protein levels of EGFRvIII vary widely across and spatially within glioblastoma tumors.[13–15] Moreover, recent observations show changes in *EGFRvIII* levels during tumor evolution after initial resection,[6,16,17] including cases with complete loss of *EGFRvIII* over time. That such a common presumed driver mutation gets lost, or levels get reduced during tumor evolution is paradoxical and will complicate targeting it for clinical benefit.

In this study, we aim to unravel *EGFRvIII*-specific mechanisms related to glioblastoma tumorigenesis. We examined *EGFRvIII* expression, its genomic breakpoints, and co-occurrence with other genetic changes using a large combined dataset.

## Methods

### Sequencing Data

Sequencing of the Intellance-2[18] (paired-end; 2 × 151 bp total RNA + paired-end; 2 × 76 bp TruSight Tumor 170 panel) and BELOB (single-end; 50 bp)[19] data was described elsewhere. For G-SAM, RNA extraction was performed using the AllPrep DNA/RNA FFPE kit or the RNeasy FFPE kit (Qiagen, Venlo, the Netherlands). G-SAM samples were

sequenced (150 bp paired-end reads) on the Illumina NovaSeq at the GIGA-Genomics Core Facility University of Liège. Each of these datasets was non-poly(A)$^+$-enriched and thus also include non-polyadenylated transcripts.[20] Raw sequencing data are available (BELOB: EGAS00001004570, Intellance-2: EGAS00001005437; G-SAM: EGAS00001005436). TCGA-GBM (poly(A)$^+$ RNA and DNA mutations) and CPCT-02 and PCAWG DNA data were obtained from their public repositories.

## Human Specimens

Tissue and metadata from the G-SAM and Intellance-2 studies were accrued through the pan-European Organisation for Research and Treatment of Cancer network.[6,18] Informed written consent was obtained from all patients. The study design was approved by the institutional review board of Erasmus MC (Rotterdam, the Netherlands), and conducted according to institutional and national regulations.

## Sequencing Data Processing

For each RNA-seq sample, FASTQ files were cleaned using *fastp* (https://github.com/OpenGene/fastp), aligned to hg19 using STAR[21] and then de-duplicated with *sambamba*. For the Dr. Disco[20] pipeline, samples were first FASTQ-level de-duplicated level using *HTStream deduper* (https://github.com/ibest/HTStream). *EGFRvIII* and *EGFRwt* expression was estimated directly from BAM files using junction-reads (https://github.com/yhoogstrate/egfr-v3-determiner v0.7.4: --spliced-reads-only). Reads considered *EGFRvIII* spanned the splice junction of exons 1-8, and reads considered *EGFRwt* exons 1-2. Samples with <10 such reads were excluded, except for TCGA-GBM, where *EGFRwt* read counts for *EGFRvIII*-negative samples were missing. Junction read counts of replicated samples were merged by summing the spliced read counts. The *EGFRvIII* percentage was defined as the average percentage when matching data from both sequencing assays were present (Intellance-2). Gene level read counts were obtained using featureCounts and Gencode v31. *EGFRvIII* counts from TCGA-GBM were taken from elsewhere.[4] Junction-counts involving non-canonical exons A, B, and C were determined using *egfr-v3-determiner* with modified exon annotations. Genomic events were taken from processed WES data or public resources (Supplementary Methods).

## Expression Analysis

Samples with an *EGFRwt* + *EGFRvIII* read count ≥10 were eligible for *EGFRvIII* status and percentage determination and for differential gene expression (DE) analysis. For DE analysis, only genes with on average ≥3 reads per sample were included. Only genes marked as "*protein_coding*" were included. DE analysis was performed using DESeq2 (Wald test),[22] in which *EGFRvIII* was excluded in *estimateSizeFactors* to avoid redundant counts. The FDR-adjusted *P*-value reflects the *q*-value. For the tests with 4 datasets combined, the intersected protein-coding genes with on average ≥3 reads per sample, per dataset, were included. Normalized expression levels were estimated using DESeq2 followed by the VST transformation (blind=TRUE) to ensure homoscedasticity.[22] A batch correction was performed for DE and for correlation analysis to correct per-dataset differences (DESeq2 for count data; limma::removeBatchEffect[23] for VST-transformed data). Volcano plots were generated with the *EnhancedVolcano* package (https://github.com/kevinblighe/EnhancedVolcano). Kaplan-Meier analysis was performed using R's *survival* package. Survival analysis on *EGFRvIII* expression was performed with a Cox Proportional Hazard survival using R's *survival* package on the normalized VST-transformed expression values. Because the Depatux-M antibody binds *EGFRvIII* with high affinity[24] and the Intellance-2 trial reported a benefit from Depatux-M in *EGFRvIII*-positive samples,[18] Depatux-M arms were excluded from survival analysis.

## Breakpoint Analyses

Non-poly(A)$^+$-enriched RNA-seq samples include relatively large proportions of intronic reads derived from actively transcribed pre-mRNA. This allows detection of genomic breakpoints when corresponding introns are sufficiently covered.[19,20] Settings for Chimeric alignment are given in Supplementary Methods.

The 100-vertebrates-*phastCons* track was obtained from UCSC and smoothened by a running mean of 200 bp fixed windows. H3K27ac Chip-Seq data were obtained from GSM3382305,[25] GSM3670052, GSM3670055, and GSM3670058.[26] Actual genomic enhancer locations were not provided in the original manuscript.[25] Their raw CRISPRi-assay data (GSM4141363 + GSM4141364) were used to reproduce their findings according to their described methodology (Supplementary Table 3).

## Exon-B Variant Experiments

To confirm the *EGFRvIII* exon-B variant, 10 samples positive for the variant (RNA-seq) with remaining isolated RNA leftover from sequencing were chosen (Supplementary Table 2). cDNA was synthesized in a buffer of 1 µl random primers, 1 µl dNTP mix, 1000 ng RNA, and 13 µl $dH_2O$. The mixture was heated to 65°C for 5 minutes and incubated on ice for 1 minute. After brief centrifugation, the contents were collected, and the following was added: 4 µl 5× First-Strand buffer, 1 µl 0.1 M DTT, 0.5 µl RNaseOUT, 1 µl Superscript III. The mixture was incubated at 25°C for 5 minutes, at 50°C for 45 minutes, and inactivated at 70°C for 15 minutes. Partial sequences spanning the exon-B splice junction were PCR-amplified using 6 primer combinations (2× exon-B, 1× exon-8, 2× exon-9). For each reaction, the buffer consisted of: 7.9 µl nuclease-free water, 3 µl 5× GoTaq buffer, 0.8 µl 10 mM dNTPs, 1 µl 10 µM forward primer, 1 µl 10 µM reverse primer, 1 µl cDNA, and 0.3 µl GoTaq polymerase. Denaturation of cDNA was performed at 98°C for 30 seconds, followed by 40 cycles of 30 seconds at 98°C, 30 seconds at 60°C, and 30 seconds at 72°C. The final extension was performed at 72°C for 5 minutes and brought

back to 12°C. Of the 10 samples, 6 showed bands of the expected size on agarose gel. Of these 6, 4 were sent out for Sanger Sequencing to Macrogen Europe B.V., Amsterdam (Supplementary Table 2). Three of the four samples showed good per-base quality. Forward and reverse reads were assembled into consensus contigs using UGENE.

Constructs were generated to evaluate the function of EGFR variants initiating from exon-B. Because exon-B lacks a translation initiation site, we generated these constructs using the first in-frame ATG in exon-2 or exon-8 (in the case of *EGFRvIII*). A total of 16 different constructs were made: those that initiated translation in exons 2 or 8 with (i) either an in-frame eGFP (located C-terminal to the transmembrane region[27]) or eGFP co-expressed via an IRES sequence; (ii) with and without the L858R activating mutation (to compare the activation state of the novel isoforms with a constitutively active isoform); and (iii) without/with a canonical Kozak sequence (to ensure optimal translation of the latter). Constructs were generated by in-fusion cloning into a piggyback vector. Constructs were stably transfected in HeLa cells, imaged using an Opera Phenix (PerkinElmer, Hamburg, Germany) high content imager and analyzed using Harmony software (PerkinElmer, Hamburg, Germany).

## Results

We have collected glioblastoma data from the following cohorts: BELOB,[19] Intellance-2,[18] G-SAM,[6] TCGA-GBM,[4] CPCT-02,[28] and PCAWG.[29] The compiled results are available as a study dataset: https://zenodo.org/record/4792445.

### Molecular Differences of EGFRvIII-Expressing Tumors

To determine *EGFRwt* (spliced across exons 1-2) and *EGFRvIII* (spliced across exons 1-8) expression, we first developed *egfr-v3-determiner* (publicly available, see Methods). Out of the 839 available RNA-seq samples, we included samples with a combined *EGFR* junction read count (spliced across exons 1-2 and 1-8) of ≥10 into our combined study RNA dataset: n = 741 from 622 patients; BELOB (n = 69/92), Intellance-2 (n = 224/239), G-SAM (n = 285/345) complemented with all primary TCGA-GBM samples (n = 163). In this combined dataset, 464/741 (62.6%) samples had *EGFR* gene amplification or upregulation if copy-number data were absent. Using the transcript-specific junction-counts, we calculated the ratio *EGFRvIII* ($\frac{count\ EGFRvIII}{count\ EGFRvIII+EGFRwt}$). Of the *EGFR*-amplified samples, 225/464 (48.5%) were considered *EGFRvIII*-expressing ($\frac{count\ EGFRvIII}{count\ EGFRvIII+EGFRwt} \geq 1\ \%$), consistent with observations in the literature.[9,30] These ratios revealed a high dynamic from 1% to 95%, consistent in all datasets (Figure 1). Lower *EGFRvIII* expression ratios were slightly over-represented (1%-10%; $P = 3.2e^{-9}$; Wilcoxon test on the first derivative of the ordered percentages). The total *EGFR* expression levels are on average lower for samples with higher *EGFRvIII* percentages, implying that *EGFRvIII* is more potent in *EGFR* signaling (Figure 2, Supplementary Figure S1D).

Several reports have indicated that *EGFRvIII* and *EGFRwt* activate different signal transduction pathways.[9,31] To assess if such differences are reflected in their transcriptomes, we performed DE analysis comparing the transcriptomes of *EGFRvIII*-positive (using 2 cutoffs: ≥1.0% or ≥10.0%) with *EGFRvIII*-negative (<1.0%) but *EGFR*-amplified tumors. Tests were performed for all 4 datasets separately, to correlate the logarithmic fold changes (LFC) of the genes between the datasets. Markedly higher LFC correlations were found across the datasets using ≥10% *EGFRvIII* as cutoff (Supplementary Figure S2), which suggests lower percentages (1-10) harbor a limited *EGFRvIII* response signal.

We therefore proceeded with the combined dataset using only ≥10% *EGFRvIII* as cutoff (n = 368) and found 213 genes significantly (*q*-value < 0.01, |LFC| > 0.5) differentially expressed (Figure 3A). They showed enrichment in genes related to microtubule-, cilium-, and axoneme-related pathways (Supplementary Figure S3).

The 187 significantly downregulated genes in ≥10% *EGFRvIII* included *CDK4* and *MDM2*, genes that are frequently hyper- and co-amplified in glioblastoma. Their observed differences were not a result of consistent down-regulation of *CDK4* or *MDM2* across all ≥10% *EGFRvIII*-positive patients but were caused by a lower proportion of tumors with extremely high *CDK4* or *MDM2* expression levels (Supplementary Figure S4A and B). Integration with copy-number data confirmed the negative association: *CDK4* or *MDM2* DNA amplifications appeared in significantly fewer tumors expressing *EGFRvIII* ($P = .007$, Fisher exact test, Supplementary Figure S4C). *TP53* mutations were indeed[32] less frequently present in *EGFR*-amplified tumors, both *EGFRvIII*-positive and -negative (Figure 1, Supplementary Figure S1). Similarly, *TACC3-FGFR3* fusions were indeed[33] exclusively present in *EGFR* non-amplified tumors. The overall transcriptome differences did not show a strong separation between *EGFRvIII*-positive and -negative tumors, indicating the overall differences are modest (Figure 3B).

Glioblastomas are classified into 3 transcriptional subtypes: mesenchymal, proneural, and classical. Classification is based on genes that are exclusively upregulated within their subtype.[34,35] The classical subtype is characterized by *EGFR* amplifications.[35] We observed that almost all classical subtype genes tend to be upregulated in *EGFRvIII*-positive tumors ($P = 3.873e^{-6}$; Fisher exact test on positive/negative LFC, Figure 3A) compared with *EGFRvIII*-negative tumors, all harboring *EGFR* amplifications. The classical subtype, therefore, is at least partly defined by *EGFRvIII*-specific signaling. While certain neuronal precursor and stem cell marker, sonic hedgehog pathway, and notch pathway member genes are highly expressed in the classical subtype,[36] these individual pathways did not differ across *EGFRvIII*-positive/-negative tumors (Supplementary Figure S5A–C). According to a pathway-based glioblastoma classification,[37] two subtypes, proliferative/progenitor (PPR) and mitochondrial (MTC), are associated with RTK pathway amplifications such as *EGFR* and *PDGFRA*. Of these, PPR is associates positively with *EGFRvIII* (Supplementary Figure S5D and E).

In addition to the DE analysis using a defined *EGFRvIII* expression cutoff, we interrogated the linear correlation between the expression of all genes to the *EGFRvIII* expression.

Neuro-Oncology



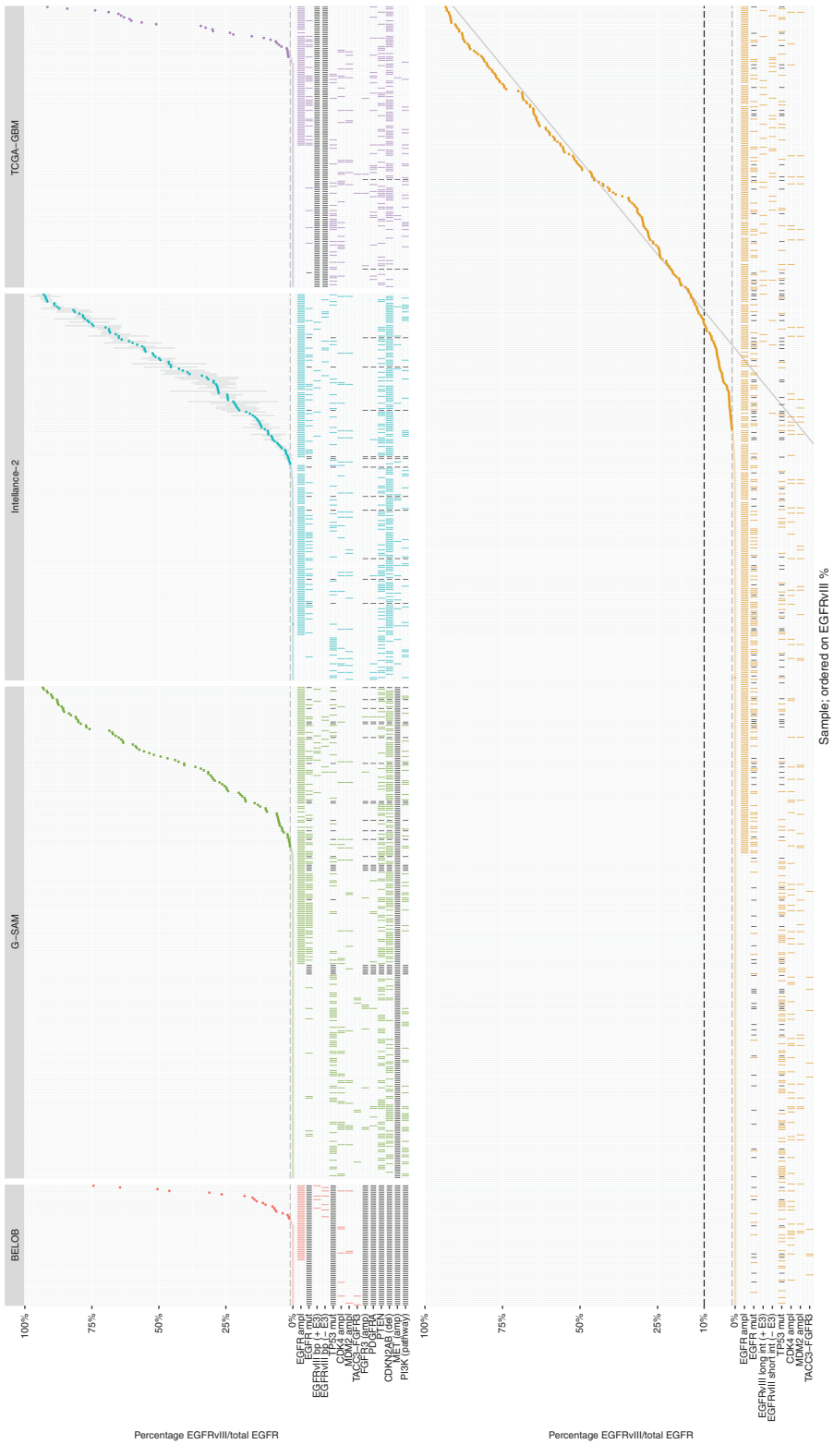


**Fig. 1** Range of *EGFRvIII* percentages relative to total *EGFR*. Results are split per dataset (top) and combined (bottom). Gray vertical lines (Intellance-2) indicate levels determined by both full and panel-based RNA-seq where the actual percentages reflect their mean. Mutation statuses are indicated underneath. N/A-values are indicated in black.

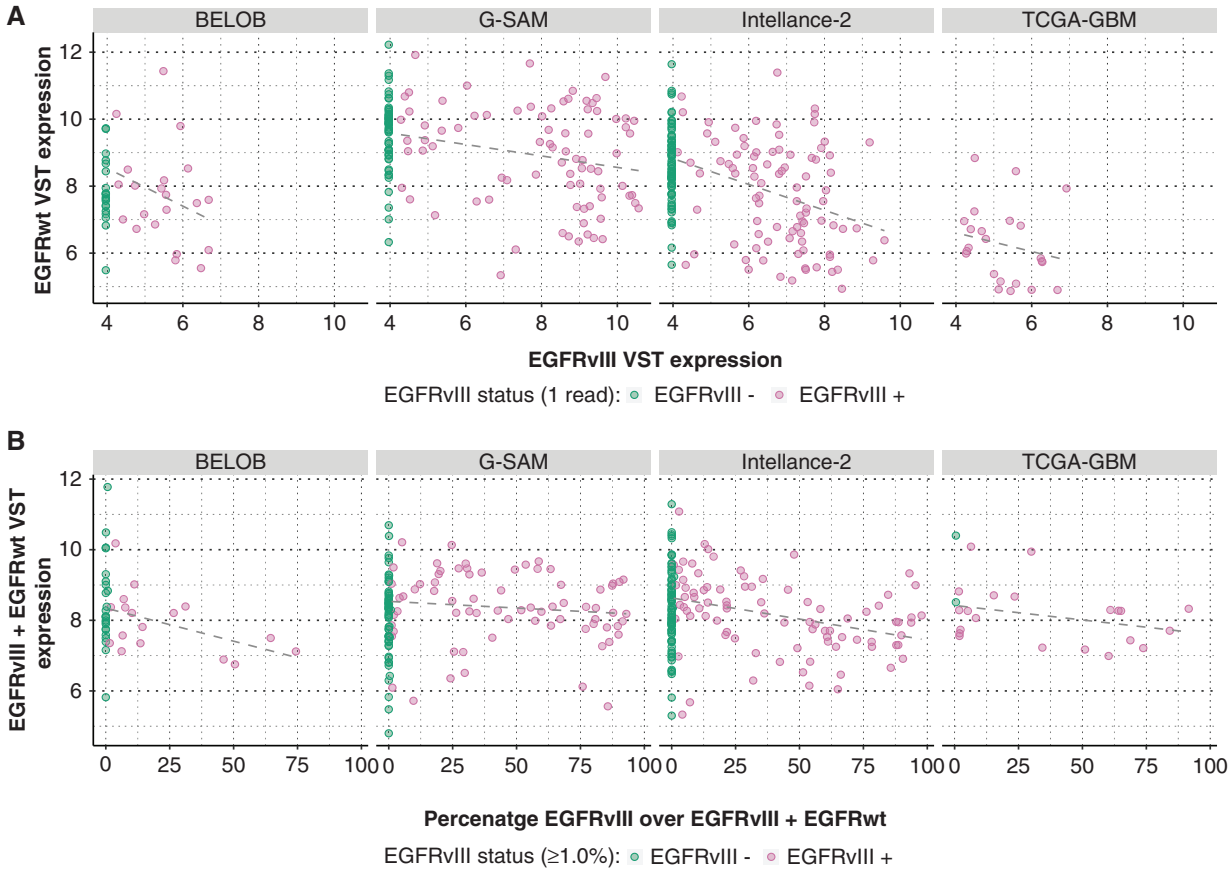


**Fig. 2** EGFRwt/EGFRvIII correlations. (A) *EGFRwt* and *EGFRvIII* correlation and (B) total *EGFR* and percentage of correlation, per dataset. (A) The correlations between *EGFRwt* and *EGFRvIII* are negative; (B) y-axis represents a surrogate for the total *EGFR* level (VST-transformed sum of *EGFRwt* + *EGFRvIII* junction-reads because the full gene *EGFR* read count is negatively affected by exons missing in *EGFRvIII*). Correlations are negative, indicating that tumors with higher proportions of *EGFRvIII* have lower levels of both variants combined.

This analysis was performed within the same ≥10% *EGFRvIII*-positive samples. *CDK4* and *MDM2* expression levels did not linearly correlate with *EGFRvIII* expression. That there is a significant difference in *CDK4* and *MDM2* expression levels across *EGFRvIII*-positive and -negative tumors while their expression levels do not correlate with *EGFRvIII*, is in concordance with the difference in hyper-amplification incidence. To identify genes that correlate differently between *EGFRvIII* and *EGFR*, we performed the same test against *EGFRwt* (Figure 3C). We then calculated per gene to what extent the correlation with *EGFRwt* and *EGFRvIII* differs, and tested which differences were beyond what may be expected by chance (Supplementary Methods). This revealed 6 additional genes that significantly differ in their correlation to *EGFRwt* in contrast to *EGFRvIII* (*NSG1*, *GALNT15*, *RFWD3*, *NCAPD3*, *ARHGEF26*, and *PHF19*; $q < 0.01$). *RFWD3* was positively correlated with *EGFRvIII* (coef = 0.33) while negatively correlated with *EGFRwt* (coef = –0.20). Similar to using a defined *EGFRvIII* expression cutoff, we found that the classical subtype genes correlate positively stronger with *EGFRvIII* compared with *EGFRwt* ($P = 1.1e^{-9}$; 2-sided *t* test on *Z*-score difference).

The difference in correlation between *EGFRvIII* and *EGFRwt* and the difference in gene expression by *EGFRvIII* presence, showed correlation (Spearman coef = 0.4, Supplementary Figure S6). For classical subtype genes, this correlation was stronger (Spearman coef = 0.7), indicating consistency in the outcome of the tests. In particular, genes that showed strong concordant results were *PHF19*, *NSG1*, and Sprouty/Spred family members *SPRED2*, *SPRY4*, and *SPRY2* (Supplementary Figure S6B). Furthermore, *PTPRZ1*, occasionally found in glioma as donor partner in fusions such as *PTPRZ1-ETV1* and *PTPRZ1-MET*,[38] positively associates with *EGFRvIII*.

## EGFRvIII Prognostic Value

There have been conflicting data on the association of *EGFRvIII* with prognosis.[9] We interrogated the patient survival between *EGFRvIII*-positive and -negative patients in the BELOB, G-SAM, and TCGA-GBM and Intellance-2 (control arm) datasets. Within patients with *EGFR*-amplified tumors, there was no significant difference in overall survival between patients with *EGFRvIII*-positive and -negative tumors (n = 327) in each dataset or combined (Figure 4, Supplementary Figure S7). There was no significant

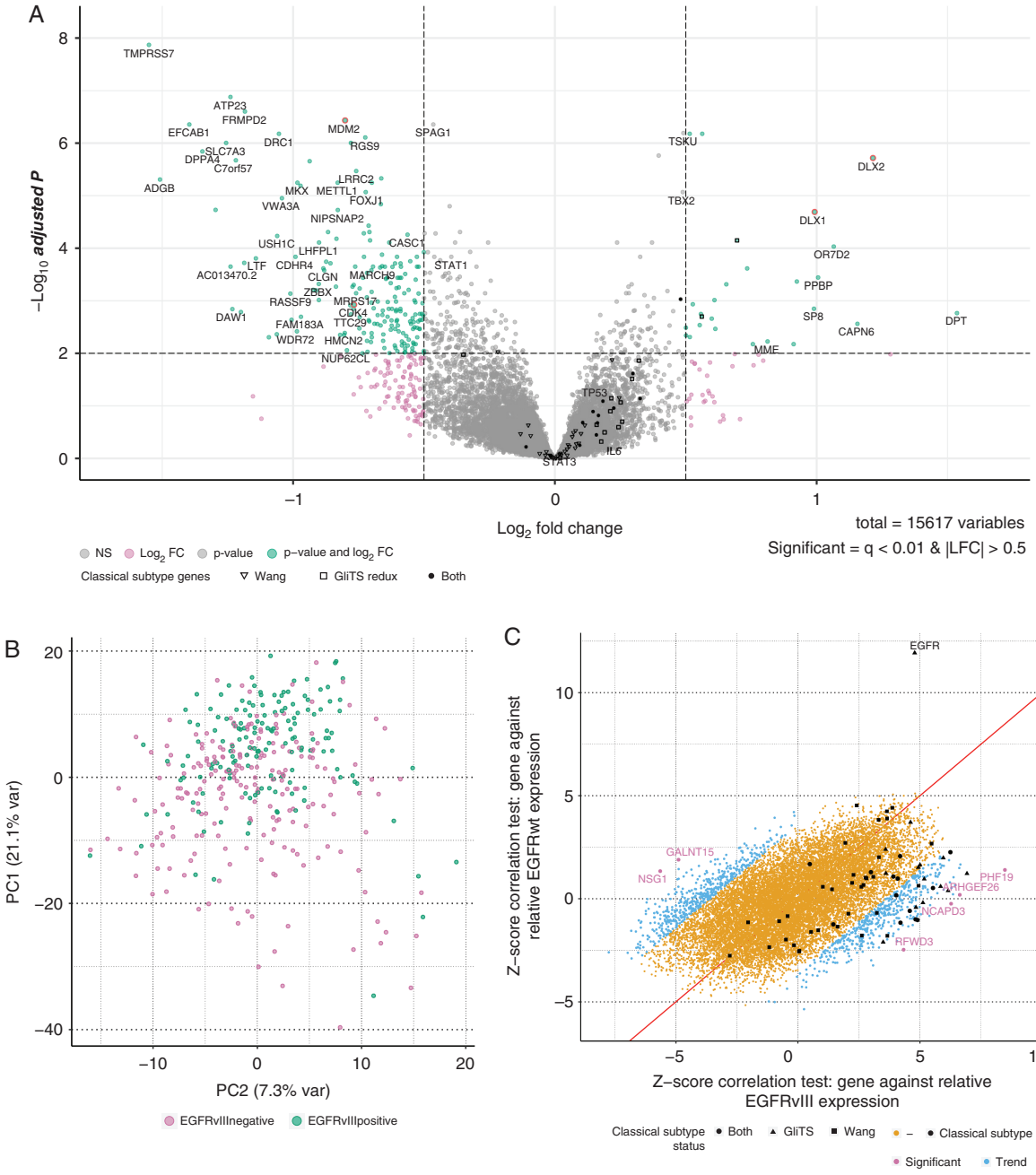


**Fig. 3** (A) DE analysis between EGFR-amplified samples with (≥10%) and without *EGFRvIII* (<1%), with batch correction for the 4 datasets (Intellance-2, G-SAM, BELOB, and TCGA-GBM). 213/15.617 protein-coding genes were differentially expressed, including *DLX1*, *DLX2*, *TSPAN31*, *TMPRSS7*, *PPBP*, and *DPT*. Classical subtype genes are marked black. Overall LFCs were more often negative while the majority of the classical subtype genes had a positive LFC. (B) First two components of a supervised principal component analysis (213 DE genes). (C) *Z*-scores of Pearson correlation tests between genes and the relative *EGFRvIII* (x-axis) and *EGFRwt* (y-axis) levels, in samples with ≥10% *EGFRvIII*. Values near 0 represent no correlation, negative values represent a negative correlation, and positive values represent a positive correlation. Classical subtype genes are marked black. Genes with a significant difference (*t* test; *q*-value < 0.01) are marked purple. Genes showing a trend (*q*-value < 0.1) are marked blue.

association between relative *EGFRvIII* expression levels and patient survival (HR: BELOB = 1.1, G-SAM = 0.96, Intellance-2 = 1.2). In summary, we found no evidence for an association of *EGFRvIII* with survival in patients with *EGFR*-amplified tumors.

## EGFRvIII Breakpoints Preferentially Retain Intronic Enhancer

With a transcription rate of 1-6 kb/min,[39] transcription of the ~120 kb *EGFR* intron-1 can take up to 2 hours. The closer

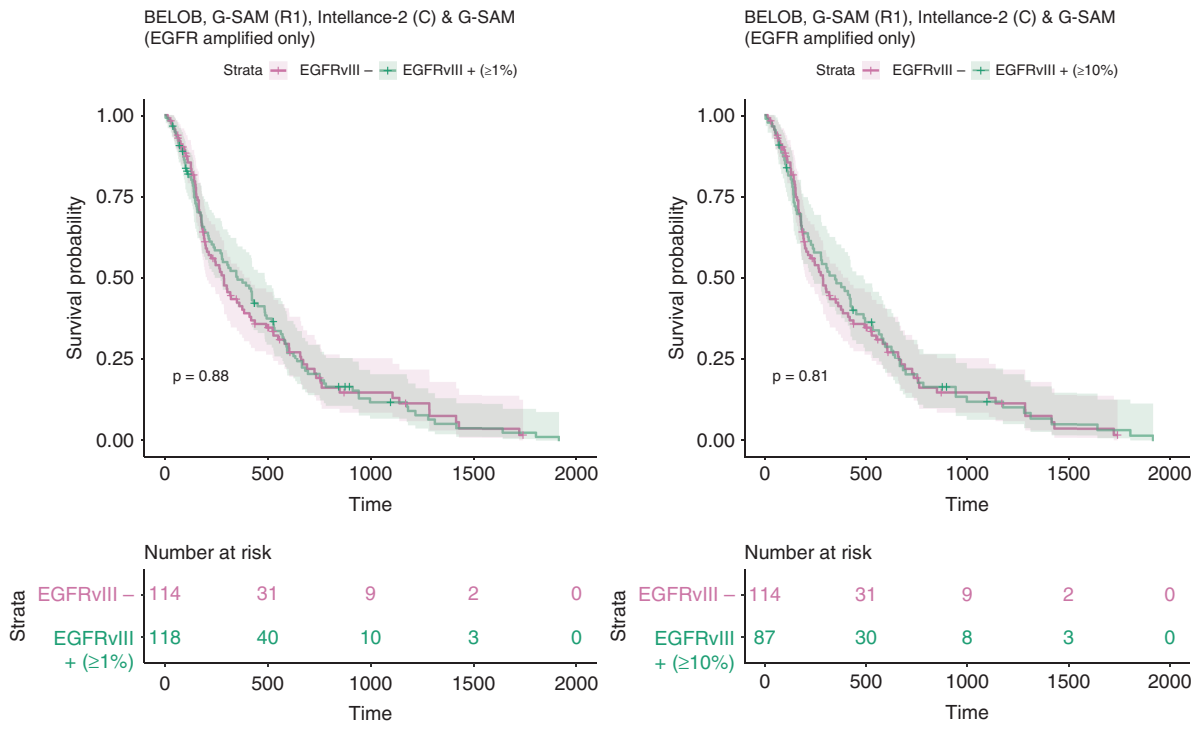


**Fig. 4** Kaplan-Meier survival plots of patients with *EGFR* amplification with/without *EGFRvIII*. Patients included were from the BELOB trial, Intellance-2 TMZ/control arm, primary G-SAM tumors, and primary TCGA-GBM tumors. Difference in patient survival between *EGFR*-amplified glioblastoma patients with/without *EGFRvIII* (≥1% and ≥10%) was not significant and neither in each dataset separately (Supplementary Figure S7).

the breakpoint of the causal *EGFRvIII* deletion is to exon-1, the shorter its intron. Given the large size of intron-1, breakpoints at the beginning of the intron (early breakpoints) may provide an energetic and temporal benefit over breakpoints at the end of the intron (late breakpoints). We screened ≥1% *EGFRvIII*-positive samples for their genomic *EGFRvIII* breakpoints based on the presence of pre-mRNA.[19,20] We found 44 breakpoints within our datasets (Supplementary Table 1; Figure 5). One sample harbored 2 unique *EGFRvIII* breakpoints. We complemented these breakpoints with those identified from CPCT-02 (8/41 patients)[28] and PCAWG (11/40 patients)[29] whole-genome sequencing datasets. In several samples, we observed multiple, unique *EGFRvIII* breakpoints (Supplementary Figure S8A) that could not have evolved from a tumor-specific ancestor *EGFRvIII* variant. In these cases, *EGFRvIII* thus has independently reoccurred within the same tumor.

Interestingly, the genomic breakpoints found in intron-1 show a difference in breakpoint density, where the region close to exon-1 contains 3.63 times fewer breakpoints per base than the region close to exon-2 ($P = 4.9e^{-13}$; Fisher exact test; decision-boundary: chr7:55.182.397). Genomic breakpoints between exons 7-8 were more uniformly distributed (Supplementary Figure S8B). The breakpoint preference in intron-1 may suggest preserving functional regions that confer a selective advantage to the tumor. Upon closer inspection, *EGFR* intron-1 contains 3 non-canonical exons[40] of which their expression is only rarely observed. We refer to these as exons A, B, and C. The *EGFRvIII* breakpoint preference region is located 3′ of exon-B (Figure 5) and thus preserves this exon at the genomic level. All datasets examined revealed junction-reads that initiated in exon-B and were spliced to exon-2 (*EGFRwt*) or exon-8 (*EGFRvIII*) (Figure 6). However, the fraction of transcripts containing exon-B was low compared to those initiating in exon-1 (≤1.05%; Supplementary Figure S8C), indicating exon-B expression is driven by a weak promoter. Transcripts spliced from exons A or C to exon-2 were extremely rare.

In samples with breakpoints retaining exon-B, a novel exon-B-exon-8 *EGFR(vIII/B)* variant is created (Figure 6). This variant was confirmed with RT-PCR in 6 out of 10 tested tumor samples (Supplementary Table 2). We verified the presence of the exon-B→exon-8→exon-9 sequence in 3 samples (GenBank: MZ484953, MZ484954, and MZ484955). *EGFR* transcripts that initiate in exon-B lack part of the extracellular domain on protein level as the translation initiation sites are located in exon-2 or exon-8. To test the potential functional role of exon-B variants, we created constructs of EGFR starting in exon-B and spliced to either exon-2 or exon-8.

Even after optimizing the Kozak sequence surrounding the translation initiation site, we failed to see the expression of "exon-B" variants in any of the 16 constructs generated. This absent expression was not due to a potential lethality of exon-B constructs as (1) RT-PCR did show expression of the *EGFR* transgene and (2) biscistronic constructs (in which eGFP was independently translated from

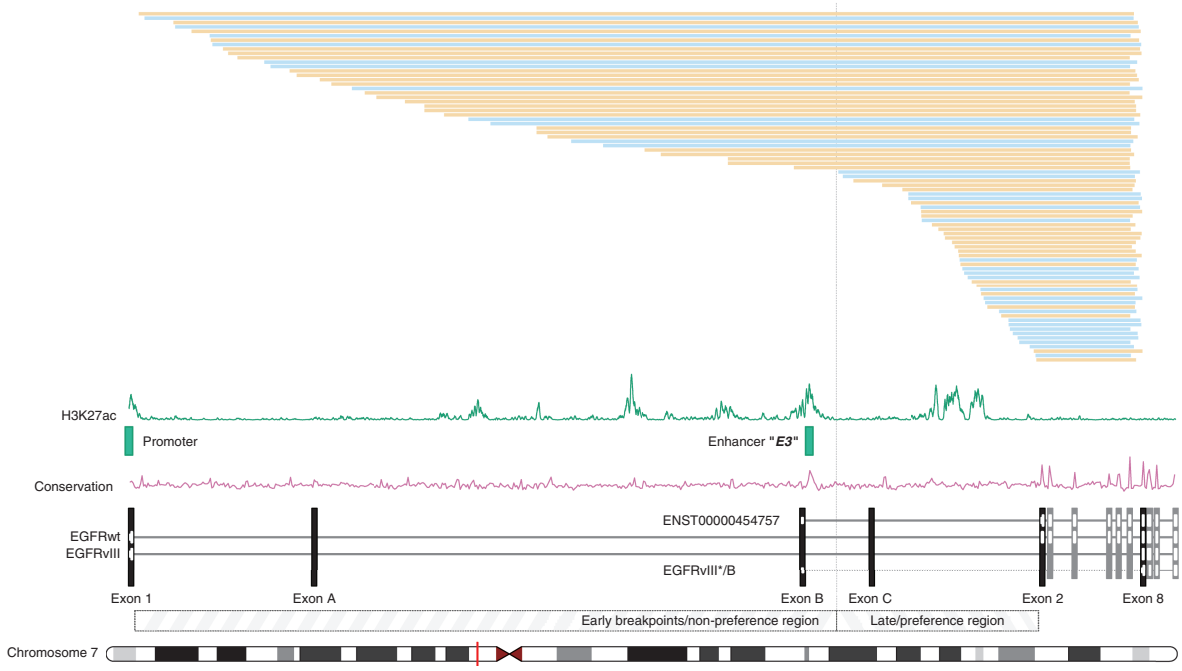


**Fig. 5** Overview of genomic *EGFR* locus (exons 1-11) and *EGFRvIII* breakpoints. From bottom to top: chr7, transcript annotations, late and early breakpoint regions, conservation (purple), H3K27ac intensity in GSC23 cells[25] (green), and the actual breakpoints (blue and mustard). Genomic *EGFRvIII* breakpoints are indicated with mustard (RNA detected) and blue (DNA detected) bars on top.

EGFR constructs as they were separated by an IRES sequence) did express eGFP. These data argue for an inferior protein translation of exon-B transcripts. Given the inadequate translation into protein combined with the low level of transcripts incorporating exon-B, we deemed it unlikely these constructs significantly impact the tumor biology.

We explored the possibility that late breakpoints retain regulatory sequences further. H3K27ac ChIP-seq data from recent studies on *EGFR* enhancers[25,26] were plotted onto the *EGFR* locus (Figure 5, Supplementary Figure S9). An enhancer, previously referred to as "E3,"[25] located just 5′ to the *EGFRvIII* breakpoint preference region and is thus more often preserved. This region is conserved across 100 vertebrates. Previous experiments using CRSIPRi demonstrated its functional relevance in cell fitness. Unfortunately, too few samples with detected breakpoints and combined RNA-seq and DNA-seq data were available to determine whether late breakpoints have a higher fractional *EGFRvIII* expression (Supplementary Figure S10).

## Discussion

*EGFR* is commonly amplified, mutated, and activated in glioblastoma, resulting in increased cell invasion and proliferation.[41] *EGFRvIII* is a specific tumor marker often present in glioblastoma, that has been intensively investigated.[9,18] Here, we report on this genomic mutation using a large glioblastoma *EGFRvIII* omics dataset. To maximize statistical power, analysis was performed across a combined cohort of 4 RNA datasets and 2 independent whole-genome sequencing datasets. Previous data on the prognostic value of *EGFRvIII* were conflicting, with some suggesting *EGFRvIII* is a negative[42,43] or a positive[44] prognostic marker, where other studies also suggested it did not affect survival.[45,46] Here, we demonstrate that within patients with *EGFR*-amplified glioblastoma, we observed no difference in survival between *EGFRvIII*-positive and -negative tumors. Because *EGFRvIII* is known to be spatially heterogeneously distributed,[13,14] *EGFRvIII*-positive tumors can, therefore, through sampling, be marked *EGFRvIII*-negative by omics analysis. Tumor sampling is therefore a limitation potentially influencing this survival analysis.

The expression levels of *EGFRvIII* and *EGFRwt* were anti-correlated and the total *EGFR* levels were generally lower when higher levels of *EGFRvIII* were present. This is in agreement with the hypothesis that *EGFRvIII* lowers the tumors' dependency on high *EGFR* amplification levels.[18]

Transcriptomes of *EGFRvIII*-positive and -negative tumors showed only minor differences (Figure 3B). A possibly related factor of this limited difference may be the ability of *EGFRvIII* to alter expression in *EGFRvIII*-negative tumor cells.[15] Within *EGFR*-amplified tumors, those with ≥10% *EGFRvIII* were found to have significantly lower expression of *CDK4* and *MDM2* due to a lower incidence of respective amplifications. This inverse correlation may point toward crosstalk or redundancy between these pathways. Of the genes correlated positively to *EGFRvIII* expression, *RFWD3* can form a complex with *MDM2*,

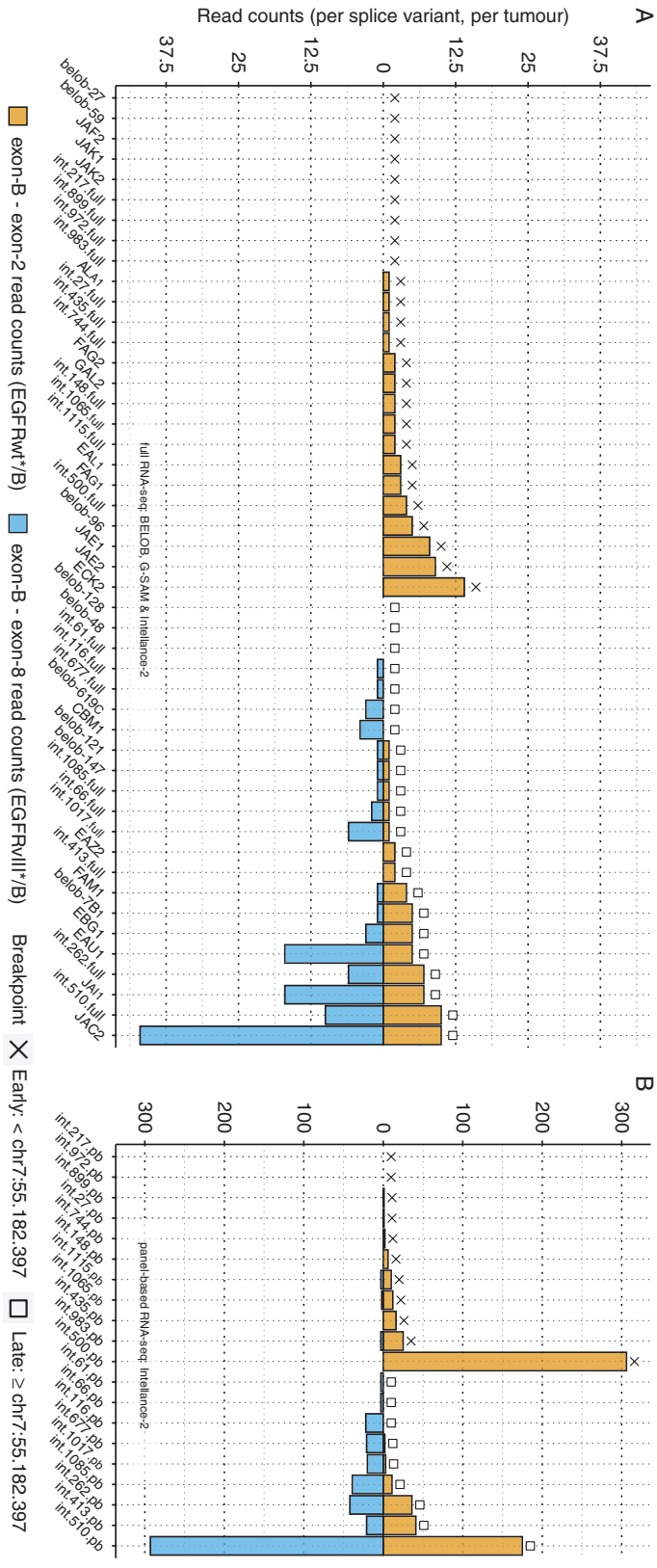


**Fig. 6** Exon-B expression. Spliced read counts for exon-B (exon-B→exon-2: bars up and exon-B→exon-8: bars down) in tumors with RNA detected genomic *EGFRvIII* breakpoint. Tumors with a "late" intron-1 breakpoint (≥chr7:55.182.397) are marked with a square and "early" with a cross. Regular (A) and high (B) depth datasets were split. *EGFRvIII* exon-B variant reads (exon-B→exon-8) are only present in tumors with a late *EGFRvIII* breakpoint, which retains exon-B.

known for regulating p53.[47] Furthermore, Sprouty/Spred family genes were consistently associated with *EGFRvIII* presence and subsequent expression and are known for their inhibiting role in Ras/Raf/ERK[48] and involvement in *EGF*/*EGFR* signaling. The presented results are not supporting the standpoint that *EGFRvIII* is causing large distinct changes in downstream gene expression compared with *EGFRwt* amplifications.

Overall, our molecular analysis demonstrated that glioblastomas expressing *EGFRvIII* show a distinct but limited difference in their transcriptome compared with *EGFRwt*. The clearest observed signal is an increased correlation with classical glioblastoma subtype genes, which may indicate that the constitutively active *EGFRvIII* is, in the context of *EGFR*-amplified glioblastoma, stronger in downstream *EGFR* signaling than (amplified) *EGFRwt*. This is in line with the lower total *EGFR* levels for tumors having higher *EGFRvIII* levels.

We found a broad range of *EGFRvIII*/total *EGFR* expression levels (1%-95%). Such range is puzzling because, if *EGFRvIII* is only a variant that is stronger in activating downstream EGFR signaling, it is possible that *EGFRvIII* would simply outcompete the *EGFRwt* ecDNA copies. This would likely take place relatively quickly since ecDNA amplifications are notorious for increasing tumor heterogeneity.[8] However, the presence of extrachromosomal *EGFRwt* copies lasts in virtually all analyzed *EGFRvIII*-positive tumors. An explanation could be that *EGFRvIII* depends on the presence of *EGFRwt*,[49] for instance, to form dimers to complete *EGFRvIII* phosphorylation[50] or in an inter-cellular context, for instance by *EGFRvIII*-dependent secretion of cytokines.[15] Such dependencies would likely come with a preferred *EGFRvIII*/*EGFRwt* ratio. Alternatively, the linear slope is indicative for an absence of selection pressure to retain *EGFRvIII* over *EGFRwt*. This absence can explain the highly heterogeneous spatial and temporal expression pattern of the mutant. It may also explain the near-identical survival between *EGFRvIII*-positive and -negative glioblastoma patients. However, if there is no selection pressure to retain *EGFRvIII*, it remains puzzling why this particular mutant is found at such a high frequency. *EGFR* signaling in glioblastomas is highly complex as the tumor can adopt various methods to enhance its pathway activation. Multiple mutations can co-exist in the same tumor, sometimes subclonal and with reported longitudinal differences, with a unique, different ligand dependency.

An earlier study proposed defining samples with a read count of at least 1% or 10% *EGFRvIII* compared with total *EGFR* as *EGFRvIII*-positive.[4] We recommend similarly rather than using the presence of any *EGFRvIII* read, as mapping artifacts and index hopping/switching derived reads are common in multiplexed RNA-seq and because higher *EGFRvIII* percentages showed a stronger response signal.

Determination of the subclonal breakpoints in pre-mRNA data was more complicated than in datasets where breakpoints were clonal.[20] Breakpoints were found predominantly in samples with high fractions of *EGFRvIII*. The median *EGFRvIII* percentage in samples with detected breakpoints was 55%, whereas 29% in samples without.

Intriguingly, we find a minority of *EGFR* transcripts starting with a cryptic exon preferentially preserved in *EGFRvIII*-expressing tumors. The first translation initiation site is located in exon-8, but the total exon-B read count is very low and, combined with a weak Kozak sequence, we did not consider this variant to be the main reason for a breakpoint preference.

Recently, the promotor and functional enhancers specifically retained in extrachromosomal *EGFR* fragments in glioblastoma and neuroblastoma cells have been interrogated.[25] These enhancers, including "E3," were discovered using 4C-seq, H3K27ac ChIP-seq, and a CRISPRi knock-down proliferation dropout assay. The E3 enhancer also showed H3K27ac in an independent dataset.[26] The preferential retention of intragenic enhancer E3 in *EGFRvIII* is in line with these observations. As the E3 enhancer is also conserved across vertebrates, it likely results in higher *EGFR* transcription rates. Unfortunately, both absolute and relative *EGFRvIII* levels differ essentially between samples, which combined with a high level of *EGFRwt* heterogeneity makes it difficult to confirm this hypothesis.

In summary, using the largest combined *EGFRvIII* omics dataset to date, we find that the expression profiles of *EGFRvIII*-positive tumors differ only marginally from *EGFRvIII*-negative tumors. The results suggest that *EGFRvIII* mainly performs a similar role as *EGFRwt* but with a stronger affinity to activate *EGFR* downstream pathways, possibly linked to persistent activity independent of ligand(s). Furthermore, genomic breakpoints in intron-1 retain an enhancer that likely increases the expression of *EGFRvIII* transcripts. In this retrospective setting, no prognostic difference was found between *EGFRvIII*-positive patients compared with those harboring *EGFRwt* amplifications. However, associations between *EGFRvIII* and genes such as *CDK4*, *MDM2*, and *PTPRZ1* suggest that the relation between *EGFR* and *EGFRvIII* is not fully understood and further research is needed, ideally to find therapies targeting both isoforms.

## Supplementary Material

Supplementary material is available at *Neuro-Oncology* online.


## Keywords

breakpoints | EGFR | EGFRvIII | glioblastoma | RNA-seq



## Funding

This study was supported by Télévie, Brussels, Belgium, AbbVie, Inc, a grant from the "Westlandse ride," the Brain Tumour Charity (grant number ET_2019_/2_10470), and Stichting STOPhersentumoren.nl 2013.



## Acknowledgments

We thank the GIGA facility of University of Liège for RNA-sequencing. This publication and the underlying study have

been made possible on the basis of data that Hartwig Medical Foundation and the Center of Personalised Cancer Treatment (CPCT) have made available. The authors thank the European Organization for Research and Treatment of Cancer for permission to use the data from EORTC studies EORTC_1410 (Intellance-2) and EORTC_1542 (G-SAM) for this research. We thank Martin E. van Royen for contributing.

**Conflict of interest statement.** None declared.

**Authorship statement.** Methodology: G.W.J., H.v.d.W., J.v.R., P.J.F., S.A.G., and Y.H.; Analysis: I.d.H., K.D., M.d.W., and Y.H.; Resources: A.H., A.M.E.W., C.W., E.F., F.Y.F.d.V., G.L., H.J.G.v.W., I.v.B, I.d.H., J.B., J.M.K., J.M.S., J.S.F, K.D., M.C.H., M.E.v.R., M.E., M.K., M.T., M.d.W., M.W., P.A.R., R.M.V., S.Le, S.Lu, T.G., V.B., and W.T.; Drafting article: H.J.G.v.W., J.v.R., K.D., P.J.F., S.A.G., and Y.H.; Funding: M.v.B. and P.J.F.

## References


1. Stupp R, Mason WP, van den Bent MJ, et al.; European Organisation for Research and Treatment of Cancer Brain Tumor and Radiotherapy Groups; National Cancer Institute of Canada Clinical Trials Group. Radiotherapy plus concomitant and adjuvant temozolomide for glioblastoma. *N Engl J Med*. 2005;352(10):987–996.
2. McLendon R, Friedman A, Bigner D, et al. Comprehensive genomic characterization defines human glioblastoma genes and core pathways. *Nature*. 2008;455(7216):1061–1068.
3. Parsons DW, Jones S, Zhang X, et al. An integrated genomic analysis of human glioblastoma multiforme. *Science*. 2008;321(5897):1807–1812.
4. Brennan CW, Verhaak RGW, McKenna A, et al. The somatic genomic landscape of glioblastoma. *Cell*. 2014;157(3):753.
5. French PJ, Eoli M, Sepulveda JM, et al. Defining EGFR amplification status for clinical trial inclusion. *Neuro Oncol*. 2019;21(10):1263–1272.
6. Draaisma K, Chatzipli A, Taphoorn M, et al. Molecular evolution of IDH wild-type glioblastomas treated with standard of care affects survival and design of precision medicine trials: a report from the EORTC 1542 study. *J Clin Oncol*. 2020;38(1):81–99.
7. Lassman AB, Aldape KD, Ansell PJ, et al. Epidermal growth factor receptor (EGFR) amplification rates observed in screening patients for randomized trials in glioblastoma. *J Neurooncol*. 2019;144(1):205–210.
8. Verhaak RGW, Bafna V, Mischel PS. Extrachromosomal oncogene amplification in tumour pathogenesis and evolution. *Nat Rev Cancer*. 2019;19(5):283–288.
9. Gan HK, Cvrljevic AN, Johns TG. The epidermal growth factor receptor variant III (EGFRvIII): where wild things are altered. *FEBS J*. 2013;280(21):5350–5370.
10. Lassman A, Pugh S, Wang T, et al. ACTR-21. A randomized, double-blind, placebo-controlled phase 3 trial of depatuxizumab mafodotin (ABT-414) in epidermal growth factor receptor (EGFR) amplified (AMP) newly diagnosed glioblastoma (nGBM). *Neuro Oncol*. 2019;21(Supplement_6):vi17.
11. Weller M, Butowski N, Tran DD, et al.; ACT IV trial investigators. Rindopepimut with temozolomide for patients with newly diagnosed, EGFRvIII-expressing glioblastoma (ACT IV): a randomised, double-blind, international phase 3 trial. *Lancet Oncol*. 2017;18(10):1373–1385.
12. Francis JM, Zhang CZ, Maire CL, et al. EGFR variant heterogeneity in glioblastoma resolved through single-nucleus sequencing. *Cancer Discov*. 2014;4(8):956–971.
13. Nathanson DA, Gini B, Mottahedeh J, et al. Targeted therapy resistance mediated by dynamic regulation of extrachromosomal mutant EGFR DNA. *Science*. 2014;343(6166):72–76.
14. Del Vecchio CA, Giacomini CP, Vogel H, et al. EGFRvIII gene rearrangement is an early event in glioblastoma tumorigenesis and expression defines a hierarchy modulated by epigenetic mechanisms. *Oncogene*. 2013;32(21):2670–2681.
15. Zanca C, Villa GR, Benitez JA, et al. Glioblastoma cellular cross-talk converges on NF-κB to attenuate EGFR inhibitor sensitivity. *Genes Dev*. 2017;31(12):1212–1227.
16. van den Bent MJ, Gao Y, Kerkhof M, et al. Changes in the EGFR amplification and EGFRvIII expression between paired primary and recurrent glioblastomas. *Neuro Oncol*. 2015;17(7):935–941.
17. Wang J, Cazzato E, Ladewig E, et al. Clonal evolution of glioblastoma under therapy. *Nat Genet*. 2016;48(7):768–776.
18. Hoogstrate Y, Vallentgoed W, Kros JM, et al. EGFR mutations are associated with response to depatux-m in combination with temozolomide and result in a receptor that is hypersensitive to ligand. *Neurooncol Adv*. 2020;2(1):vdz051.
19. Erdem-Eraslan L, van den Bent MJ, Hoogstrate Y, et al. Identification of patients with recurrent glioblastoma who may benefit from combined bevacizumab and CCNU therapy: a report from the BELOB trial. *Cancer Res*. 2016;76(3):525–534.
20. Hoogstrate Y, Komor MA, Riet J Van, et al. Detection of fusion transcripts and their genomic breakpoints from RNA sequencing data. *bioRxiv*. 2021:1–27. doi:10.1101/2021.05.17.441778.
21. Dobin A, Davis CA, Schlesinger F, et al. STAR: ultrafast universal RNA-seq aligner. *Bioinformatics*. 2013;29(1):15–21.
22. Love MI, Huber W, Anders S. Moderated estimation of fold change and dispersion for RNA-seq data with DESeq2. *Genome Biol*. 2014;15(12):550.
23. Ritchie ME, Phipson B, Wu D, et al. limma powers differential expression analyses for RNA-sequencing and microarray studies. *Nucleic Acids Res*. 2015;43(7):e47.
24. Reilly EB, Phillips AC, Buchanan FG, et al. Characterization of ABT-806, a humanized tumor-specific anti-EGFR monoclonal antibody. *Mol Cancer Ther*. 2015;14(5):1141–1151.
25. Morton AR, Dogan-Artun N, Faber ZJ, et al. Functional enhancers shape extrachromosomal oncogene amplifications. *Cell*. 2019;179(6):1330–1341.e13.
26. Jameson NM, Ma J, Benitez J, et al. Intron 1-mediated regulation of EGFR expression in EGFR-dependent malignancies is mediated by AP-1 and BET proteins. *Mol Cancer Res*. 2019;17(11):2208–2220.
27. Erdem-Eraslan L, Gao Y, Kloosterhof NK, et al. Mutation specific functions of EGFR result in a mutation-specific downstream pathway activation. *Eur J Cancer*. 2015;51(7):893–903.
28. Priestley P, Baber J, Lolkema MP, et al. Pan-cancer whole-genome analyses of metastatic solid tumours. *Nature*. 2019;575(7781):210–216.
29. Campbell PJ, Getz G, Korbel JO, et al. Pan-cancer analysis of whole genomes. *Nature*. 2020;578(7793):82–93.
30. Lassman AB, van den Bent MJ, Gan HK, et al. Safety and efficacy of depatuxizumab mafodotin + temozolomide in patients with EGFR-amplified, recurrent glioblastoma: results from an international phase I multicenter trial. *Neuro Oncol*. 2019;21(1):106–114.
31. Tanaka K, Babic I, Nathanson D, et al. Oncogenic EGFR signaling activates an mTORC2-NF-κB pathway that promotes chemotherapy resistance. *Cancer Discov*. 2011;1(6):524–538.
32. Watanabe K, Tachibana O, Sata K, Yonekawa Y, Kleihues P, Ohgaki H. Overexpression of the EGF receptor and p53 mutations are mutually

exclusive in the evolution of primary and secondary glioblastomas. *Brain Pathol.* 1996;6(3):217–223; discussion 23.

33. Di Stefano AL, Picca A, Saragoussi E, et al.; TARGET study group. Clinical, molecular, and radiomic profile of gliomas with FGFR3-TACC3 fusions. *Neuro Oncol.* 2020;22(11):1614–1624.
34. Wang Q, Hu B, Hu X, et al. Tumor evolution of glioma-intrinsic gene expression subtypes associates with immunological changes in the microenvironment. *Cancer Cell.* 2017;32(1):42–56.e6.
35. Orzan F, Pagani F, Cominelli M, et al.; on behalf of the Neuro-Oncology group of Spedali Civili of Brescia. A simplified integrated molecular and immunohistochemistry-based algorithm allows high accuracy prediction of glioblastoma transcriptional subtypes. *Lab Invest.* 2020;100(10):1330–1344.
36. Verhaak RG, Hoadley KA, Purdom E, et al.; Cancer Genome Atlas Research Network. Integrated genomic analysis identifies clinically relevant subtypes of glioblastoma characterized by abnormalities in PDGFRA, IDH1, EGFR, and NF1. *Cancer Cell.* 2010;17(1):98–110.
37. Garofano L, Migliozzi S, Oh YT, et al. Pathway-based classification of glioblastoma uncovers a mitochondrial subtype with therapeutic vulnerabilities. *Nat Cancer.* 2021;2(2):141–156.
38. Matjašič A, Zupan A, Boštjančič E, Pižem J, Popović M, Kolenc D. A novel PTPRZ1-ETV1 fusion in gliomas. *Brain Pathol.* 2020;30(2):226–234.
39. Jonkers I, Lis JT. Getting up to speed with transcription elongation by RNA polymerase II. *Nat Rev Mol Cell Biol.* 2015;16(3):167–177.
40. Ota T, Suzuki Y, Nishikawa T, et al. Complete sequencing and characterization of 21,243 full-length human cDNAs. *Nat Genet.* 2004;36(1):40–45.
41. Talasila KM, Soentgerath A, Euskirchen P, et al. EGFR wild-type amplification and activation promote invasion and development of glioblastoma independent of angiogenesis. *Acta Neuropathol.* 2013;125(5):683–698.
42. Feldkamp MM, Lala P, Lau N, Roncari L, Guha A. Expression of activated epidermal growth factor receptors, Ras-guanosine triphosphate, and mitogen-activated protein kinase in human glioblastoma multiforme specimens. *Neurosurgery.* 1999;45(6):1442–1453.
43. Shinojima N, Tada K, Shiraishi S, et al. Prognostic value of epidermal growth factor receptor in patients with glioblastoma multiforme. *Cancer Res.* 2003;63(20):6962–6970.
44. Montano N, Cenci T, Martini M, et al. Expression of EGFRvIII in glioblastoma: prognostic significance revisited. *Neoplasia.* 2011;13(12):1113–1121.
45. Heimberger AB, Hlatky R, Suki D, et al. Prognostic effect of epidermal growth factor receptor and EGFRvIII in glioblastoma multiforme patients. *Clin Cancer Res.* 2005;11(4):1462–1466.
46. van den Bent MJ, Brandes AA, Rampling R, et al. Randomized phase II trial of erlotinib versus temozolomide or carmustine in recurrent glioblastoma: EORTC brain tumor group study 26034. *J Clin Oncol.* 2009;27(8):1268–1274.
47. Fu X, Yucer N, Liu S, et al. RFWD3-Mdm2 ubiquitin ligase complex positively regulates p53 stability in response to DNA damage. *Proc Natl Acad Sci U S A.* 2010;107(10):4579–4584.
48. Kawazoe T, Taniguchi K. The Sprouty/Spred family as tumor suppressors: coming of age. *Cancer Sci.* 2019;110(5):1525–1535.
49. Zadeh G, Bhat KP, Aldape K. EGFR and EGFRvIII in glioblastoma: partners in crime. *Cancer Cell.* 2013;24(4):403–404.
50. Li L, Chakraborty S, Yang CR, et al. An EGFR wild type-EGFRvIII-HB-EGF feed-forward loop regulates the activation of EGFRvIII. *Oncogene.* 2014;33(33):4253–4264.